Absence of genotoxicity following pulmonary exposure to metal oxides of copper, tin, aluminum, zinc, and titanium in mice

Gutierrez, Claudia Torero; Hadrup, Niels; Loizides, Charis; Hafez, Iosif; Biskos, George; Roursgaard, Martin; Saber, Anne Thoustrup; Møller, Peter; Vogel, Ulla

DOI
10.1002/em.22634

Publication date
2024

Document Version
Final published version

Published in
Environmental and Molecular Mutagenesis

Received: 13 June 2024 | Revised: 11 September 2024 | Accepted: 16 September 2024

DOI: 10.1002/em.22634

Environmental and Molecular Mutagenesis | Environmental Mutagenesis and Genomics Society | WILEY

RESEARCH ARTICLE

Absence of genotoxicity following pulmonary exposure to metal oxides of copper, tin, aluminum, zinc, and titanium in mice

Claudia Torero Gutierrez[1,2] | Niels Hadrup[1,3] | Charis Loizides[4] | Iosif Hafez[4] | George Biskos[4,5] | Martin Roursgaard[2] | Anne Thoustrup Saber[1] | Peter Møller[2] | Ulla Vogel[1,6]

[1]National Research Centre for the Working Environment, Copenhagen Ø, Denmark

[2]Section of Environmental Health, Department of Public Health, University of Copenhagen, Copenhagen, Denmark

[3]Research group for risk-benefit, National Food Institute, Technical University of Denmark

[4]Climate and Atmosphere Research Centre, The Cyprus Institute, Nicosia, Cyprus

[5]Faculty of Civil Engineering and Geosciences, Delft University of Technology, Delft, The Netherlands

[6]National Food Institute, Technical University of Denmark, Kgs. Lyngby, Denmark

Correspondence
Ulla Vogel, National Research Centre for the Working Environment, Lersø Parkallé 105, DK-2100 Copenhagen Ø, Denmark.
Email: ubv@nfa.dk

Funding information
Danish Government

Accepted by: K. Broberg

Abstract

Inhalation of nanosized metal oxides may occur at the workplace. Thus, information on potential hazardous effects is needed for risk assessment. We report an investigation of the genotoxic potential of different metal oxide nanomaterials. Acellular and intracellular reactive oxygen species (ROS) production were determined for all the studied nanomaterials. Moreover, mice were exposed by intratracheal instillation to copper oxide (CuO) at 2, 6, and 12 μg/mouse, tin oxide (SnO_2) at 54 and 162 μg/mouse, aluminum oxide (Al_2O_3) at 18 and 54 μg/mouse, zinc oxide (ZnO) at 0.7 and 2 μg/mouse, titanium dioxide (TiO_2) and the benchmark carbon black at 162 μg/mouse. The doses were selected based on pilot studies. Post-exposure time points were 1 or 28 days. Genotoxicity, assessed as DNA strand breaks by the comet assay, was measured in lung and liver tissue. The acellular and intracellular ROS measurements were fairly consistent. The CuO and the carbon black bench mark particle were potent ROS generators in both assays, followed by TiO_2. Al_2O_3, ZnO, and SnO_2 generated low levels of ROS. We detected no increased genotoxicity in this study using occupationally relevant dose levels of metal oxide nanomaterials after pulmonary exposure in mice, except for a slight increase in DNA damage in liver tissue at the highest dose of CuO. The present data add to the body of evidence for risk assessment of these metal oxides.

KEYWORDS
Al, comet assay, Cu, Sn, Ti, Zn

1 | INTRODUCTION

Metal oxide nanomaterials are already employed in many commercial products, including gas sensors, batteries, and solar cells, while they are readily employed by the industry for catalysis and energy conversion (Chavali & Nikolova, 2019). During the production and use of these materials, occupational exposure may occur. Therefore, it is important to determine the critical effects of these materials and the exposure levels at which they occur. Genotoxicity and carcinogenicity are important endpoints to consider in this aspect as cancer is major

TABLE 1 Physicochemical characteristics of the studied metal oxides and carbon black.

Name	Primary particle size (nm) (±SD)	Specific surface area (m^2/g)	Z average size (nm)	Polydispersity index
ZnO	5.7 ± 3.8	15.2	151, at 0.04 mg/mL	0.31
CuO	7.8 ± 6.8	124	146, at 0.24 mg/mL	0.24
Al_2O_3	5.5 ± 5.5	276	95, at 1.08 mg/mL	0.50
SnO_2	4.5 ± 2.3	165	105, at 3.24 mg/mL	0.50
TiO_2	6.6 ± 4.1	297	225, at 0.36 mg/mL	0.44
Carbon black	14	295–338	80 at 3.24 mg/mL	0.16

Note: SD is an abbreviation for standard deviation. Data were previously published in (Gutierrez et al., 2023).

disease limiting human life expectancy. To our knowledge, there is limited knowledge on the genotoxicity of metal oxide nanomaterials following pulmonary exposure. The genotoxicity of copper oxide (CuO) nanoparticles has been investigated only in one study where weak genotoxic effects were observed (Hadrup et al., 2021), while three studies focusing on zinc oxide (ZnO) have reported contradicting results (Hadrup et al., 2019; Larsen et al., 2016; Saber et al., 2022). For TiO_2 nanoparticles, pulmonary exposure studies have shown that some types of TiO_2 can have genotoxic effects (Hadrup et al., 2017; Han et al., 2020; Larsen et al., 2016; Li et al., 2018; Lindberg et al., 2012; Saber, Jacobsen, et al., 2012; Wallin et al., 2017). Studies on the genotoxic effects of tin dioxide (SnO_2) and aluminum oxide (Al_2O_3) nanomaterials appear to be absent. In the current study, we investigated the genotoxicity of five metal oxide nanomaterials after pulmonary exposure, in terms of DNA strand break levels using the comet assay.

2 | MATERIALS AND METHODS

2.1 | Description of nanomaterials and their dispersion in exposure media

The ZnO, CuO, Al_2O_3, SnO_2 and TiO_2 nanomaterials were produced by spark ablation as described in previously reported studies (Feng et al., 2015; Pfeiffer et al., 2015; Schwyn et al., 1988). Their primary particle sizes and specific surface areas are provided in Table 1. Carbon Black Printex-90 was used as a benchmark nanomaterial that was kindly provided by DeGussa, Germany. For the animal study, the nanomaterials were dispersed in 2% serum from mice of the same strain as previously described (Hadrup et al., 2017). In short, the suspensions were placed in ice baths on which they were sonicated for 16 min with a 13 nm disruptor horn equipped Branson Sonifier (Prod. no. disruptor horn: 101-147-037, Prod. No. Sonifier: S-450D, Branson Ultrasonics Corp., Danbury, USA). Afterwards, suspensions for the lower dose group were prepared by subsequent threefold dilutions. These diluted suspensions were sonicated for four additional minutes prior to use. The vehicle (2% mouse serum) without nanomaterials for control exposure underwent the same treatment. The suspensions were administered to the animals within 1 h after sonication.

Dynamic light scattering (DLS) was used to determine the hydrodynamic size distributions of particle suspensions. This was done on a Malvern Zetasizer Nano ZS (Malvern Instruments, UK) with a temperature of 25°C. Dispersion Technology Software v5.0 (Malvern Instruments, UK) was used for data analysis, and the hydrodynamic size was calculated by use of a dispersion refractive index of 1.33 and viscosity set to 1.12 cP. The material refractive index was set to 1.59 for CuO, Al_2O_3, and SnO_2, 2.49 for TiO_2, and 2.02 for ZnO and carbon black; the material absorption value was set to 0.01 for CuO, Al_2O_3, and SnO_2, 0.4 for ZnO, 0.1 for TiO_2, and 2 for carbon black.

2.2 | Cell culturing and measurement of cytotoxicity in vitro

The acute monocytic leukemia THP-1 cell line was used for all the cytotoxicity tests. THP-1 cells were cultured in RPMI 1640 supplemented with 10% fetal bovine serum (FBS) (Gibco), 1% HEPES, 1% sodium pyruvate, and 0.1% gentamicin. The nanomaterials (ZnO, CuO, Al_2O_3, SnO_2, TiO_2, and Printex 90) were dispersed in sterile water with 2% FBS to reach a stock concentration of 1 mg/mL. Before their use, the particle suspensions were sonicated on ice for 16 min (cycling between 10 s on and 10 s off) using a Branson Digital Sonifier S-450D (Branson Ultrasonics Corp., USA).

The nanomaterial-induced cytotoxicity was assessed by measuring cell growth after direct exposure to the materials. This method quantifies cell numbers after exposure, and albeit being simple, it provides an impression of the status of a cell population. For this, THP-1 cells were seeded in a 24-well plate at a density of 2.0×10^4 cells/well. Nanomaterial suspensions were prepared from the stock suspension in RPMI 1640 medium, added to the cell suspension to reach concentrations of 0, 25, 50, and 100 μg/mL, and incubated at 37°C and 5% CO_2. After 24 h, the cell suspensions were transferred to centrifuge tubes, centrifuged for 5 min at 300 g, re-suspended in RPMI 1640 medium and reseeded in a 24-well plate. Cell numbers were obtained by a Casy-1 Counter TT (Schärfe Systems, Germany) immediately after reseeding, 24 and 48 h after reseeding, which represented 24, 48, and 72 h after exposure to the nanomaterials. This experiment was performed three times independently.

2.3 | Reactive oxygen species (ROS) production

The nanomaterials' potential to induce oxidative stress was assessed by quantifying the production of ROS. The 2′,7′-dichlorodihydrofluorescein diacetate (DCFH-DA) assay was used under cellular and acellular conditions. The measurement of acellular ROS production assesses the intrinsic nanomaterial capacity of producing ROS, while the cellular measurement, where THP-1 cells are directly exposed to the nanomaterials, includes also intracellular sources of ROS and antioxidant mechanisms. This assay measures ROS by fluorescence; when DCFH-DA enters the cells, it is deacetylated to DCFH and later oxidized by ROS to 2′,7′-dichlorofluorescein (DCF), which is a fluorescent molecule. In the absence of cells, DCFH-DA has to first be deacetylated with NaOH. In the cellular setup, THP-1 cells were incubated in 10 μM DCFH-DA for 15 min at 37°C. Following that, cells were centrifuged and re-suspended in Hank's balanced saline solution (HBSS). THP-1 cells were then seeded in a black 96-well plate at 5.0×10^4 cells/well. Nanomaterial suspensions were prepared in HBSS to obtain concentrations of 0.8, 1.6, 3.2, 6.3, 12.5, 25, 50 and 100 μg/mL and added to the THP-1 cells in triplicates. In the case of acellular ROS, a solution of 1 mM DCFH-DA was deacetylated using 0.01 M NaOH for 30 min at room temperature and later diluted to 10 μM with HBSS. Nanomaterial suspensions were added in triplicates to a black 96-well plate, followed by a DCFH solution. The same concentrations of nanomaterials as for the cellular setup were used. For cellular and acellular ROS, plates were incubated for 3 h at 37°C and 5% CO_2, after which fluorescence was measured using a Fluoroskan Ascent FL spectrophotometer (Thermo Scientific) at 485 and 538 nm. Three independent experiments were performed for acellular and cellular ROS measurements. Results are reported as fold differences relative to the control (0 μg/mL). In addition, we have reported the initial slope of the ROS production, based on linear regression in the concentration interval between 0 and 6.3 μg/mL. In this interval, the ROS production is relatively linear with concentration and neither plateau (possibly due to limitation of the probe) nor decreased levels (putatively due to interference between particles and emitted fluorescence in the medium) are not observed.

2.4 | Animal procedures

The animal study was reported previously (Gutierrez et al., 2023). In brief, female C57BL/6J mice, 7-week old were obtained from Janvier (France) and randomly distributed into cages. Six animals were housed per cage in the metal oxide groups ($N = 6$), while vehicle control animals were housed in groups of four animals per cage ($N = 4$). Four control animals were exposed on the same day as each metal oxide group, except for the control group for the highest dose of CuO, where six animals were used as vehicle control. In total, 184 animals were used. The mice were allowed to acclimatize for 1 week and then exposed to the test materials by a single intratracheal instillation as described previously (Jackson et al., 2011) and followed for 1 or 28 days post-exposure.

The metal oxide groups were exposed on separate days, and each metal oxide group was exposed alongside 4 or 6 vehicle controls as described above. Thus, the 28-day post-exposure periods for the different metal oxides overlapped. All vehicle controls obtained were pooled for statistical analyses ($N = 26$). Mice were kept in polypropylene cages in Enviro-Dri bedding (Brogaarden, Gentofte, Denmark). Hides and wood blocks served as enrichment and were from Mouse House (Scanbur, Karlslunde, Denmark) and Brogaarden (Gentofte, Denmark), respectively. The animals had ad libitum access to feed (Altromin prod. no. 1324, Christian Petersen, Denmark) and tap water. Room temperature was 20 ± 2°C, and the humidity 50 ± 20%. The mice were kept under a 12 h light:12 h dark cycle (from 6:00 a.m. to 6:00 p.m.). The tested doses were: CuO at 2, 6 and 12 μg/mouse, tin oxide (SnO_2) at 54 and 162 μg/mouse, aluminum oxide (Al_2O_3) at 18 and 54 μg/mouse, zinc oxide (ZnO) at 0.7 and 2 μg/mouse, titanium dioxide (TiO_2) and the benchmark carbon black at 162 μg/mouse Doses of CuO, Al_2O_3 and SnO_2 were set based on a dose-finding pilot study. For CuO, we first tested a dose of 6 μg/animal in one mouse. After 1 day, the mouse did not show any symptoms of suffering. For a second trial, the same concentration was used on three mice, two of which were followed for 3 days. The mice were warm and active. Afterwards, two higher doses were tested: 12 and 18 μg/animal. These dose levels were used in one mouse each, which was followed for 1 day. Both mice were warm and active. For SnO_2, two pilot exposures were also carried out. During the first pilot exposure, 25 μg/animal was tested in one mouse followed for 1 day. The mice was active with no sign of suffering. For the second trial, the dose was increased to 54 and 162 μg/animal, with one animal at each dose level. The mice were warm and active. Al_2O_3 was tested in two dose levels in the first pilot exposure: 54 and 162 μg/animal, using one mouse per dose. Both mice were active following exposure, however after some hours, they were not as active as other mice. In addition, the mouse exposed to the higher concentration lost around 14% of its weight. During a second trial, three mice were exposed to 54 μg/animal and followed for 3 days. All mice seemed active during all days. The dose levels of ZnO, TiO_2 and carbon black were based on previous studies (Bourdon et al., 2012; Danielsen et al., 2020; Hadrup et al., 2019; Jacobsen et al., 2015). The mice were euthanized by exsanguination after intraperitoneal injection of ZRF consisting of Zoletil 100 (Zolazepam 250 mg/mL and Tiletamine 250 mg/mL), Xysol (Xylazine 20 mg/mL), and Fentadon (Fentanyl 50 μg/mL) given in sterile saline 0.1 mL/10 g bw. The animal procedures complied with the EC Directive 86/609/EEC and Danish law regulating experiments with animals (The Danish Ministry of Justice, Animal Experiments Inspectorate permission 2020-15-0201-0485), and were approved by the local animal ethical committee.

2.5 | Determination of DNA strand breaks by the comet assay

The levels of DNA strand breaks were measured in lung and liver tissue by the comet assay. Automated scoring was done in the IMSTAR

PathFinder system as detailed previously (Jackson et al., 2013). In short, the lung and liver samples were excised from the carcass and ~20 to 40 mg of each tissue were cut into pieces of 3 × 3 × 3 mm. The samples were put in NUNC cryotubes and frozen in liquid N_2 before storage at −80°C until analysis. For the comet assay, the frozen samples were pressed through a stainless steel cylindrical sieve (diameter 0.5 cm, mesh size 0.4 mm) into 0.5 to 2 mL of ice-cold Merchant's medium (0.14 M NaCl, 1.47 mM KH_2PO_4, 2.7 mM KCl, 8.1 mM Na_2HPO_4, 10 mM Na_2EDTA, pH 7.4) and then placed on ice before being embedded in 0.7% agarose and loaded onto a Trevigen Comet Slide (Trevigen, Gaithersburg, MD, USA). The slide was incubated for 24 h with 4°C cold lysing buffer (2.5 M NaCl, 10 mM Tris, 100 mM sodium-ethylenediaminetetraacetic acid (EDTA), 1% sodium sarcosinate, 10% DMSO, 1% Triton X-100, pH 10). The slides were then rinsed for 5 min in cold electrophoresis buffer, and placed in an electrophoresis chamber where they underwent alkaline treatment with ice-cold electrophoresis buffer (0.3 M NaOH, 1 mM sodium-EDTA, pH 13.2) for 35 min. The electrophoresis was conducted for 25 min at 38 V (1.2 V/cm across the electrophoresis tank between the anode and cathode) after which the slides were rinsed twice for 5 min in neutralization buffer (0.4 M Tris, pH 7.5). Fixation was done for 5 min with 96% ethanol followed by 15 min at 45°C. The cell nuclei were stained with SYBR Green in TE buffer (10 mM Tris–HCl, 1 mM EDTA, pH 7.6). Scoring was done with the IMSTAR PathFinder™ system. The percentage of fluorescence in the comet tail (% tail DNA) served as the measure of DNA strand breaks. The IMSTAR PathFinderTM system calculates the mean %Tail DNA from all measurable comets in the gel. Negative and positive controls were included on all slides, non-exposed A549 lung epithelial cells were used as negative controls, while A549 cells exposed to 30 μM H_2O_2 for 30 min were used as positive controls.

2.6 | Statistical analyses

Statistical analysis was carried out using the Graph Pad Prism 7.02 software package (Graph Pad Software Inc., La Jolla, CA, USA). In vitro (i.e., cell growth and ROS production) and in vivo results were analyzed with one-way and two-way ANOVA, respectively. The Brown-Forsythe test was used to test the heterogeneity of variance between groups, and the normal distribution of residuals was assessed by QQ plots. Sidak's post hoc test was used to determine differences between groups in datasets that showed statistical significance ($p < .05$) in the overall ANOVA. Likewise, estimation of effect size and 95% confidence interval (95% CI) are based on Sidak's post hoc test. Results are presented as mean ± standard deviation.

3 | RESULTS

3.1 | Physicochemical characterization

Primary particle size, specific surface area, *Z* average size and polydispersity index data for the particle suspensions are provided in Table 1. Of the studied nanomaterials, ZnO and CuO were regarded as highly soluble, Al_2O_3 as lowly soluble and SnO_2, TiO_2 and carbon black as insoluble in lung tissue (Gutierrez et al., 2023; Hadrup et al., 2023). Details of the physicochemical characteristics of the metal oxides are described in our earlier work (Gutierrez et al., 2023).

3.2 | ROS production

ROS generation was measured as a marker of particle reactivity. First, cell growth was measured to assess the effects of the nanomaterials on growth rate or possible cytotoxic effects on THP-1 cells. The cell numbers were measured following exposure to different concentrations of nanomaterials and at different time points after removing them (Figure S1). Reduced cell numbers were observed after exposure to ZnO and CuO for 48 and 72 h, and Al_2O_3 for 72 h. Thus, the largest effects on growth rate were observed for the highly soluble ZnO and CuO particles, followed by the less soluble Al_2O_3. No effect on growth rate was seen for the insoluble nanomaterials.

The generation of ROS was measured in acellular and cellular setups, following 3 h of exposure to the nanomaterials (Figure 1, and Figures S2 and S3). The statistical analysis showed a significant interaction between exposure and concentration on acellular ROS production levels ($p < .001$), as well as statistically significant main effects of the concentration ($p < .001$) and type of nanomaterial ($p < .001$). For the latter main effect, the magnitude of acellular ROS production had the following order: CuO > Carbon black > TiO_2 > other particles [ZnO, Al_2O_3, and SnO_2]. Concentration-dependent ROS generation was observed for CuO and TiO_2 and for carbon black at low concentrations (≤6.3 μg/mL). ROS generation potential was quantified as the initial slopes of the concentration-response curves (Table 2).

3.3 | Levels of DNA strand breaks in mice

Female mice were exposed by intratracheal instillation to the ZnO, CuO, Al_2O_3, SnO_2, TiO_2, or carbon black nanomaterials and followed for 1 or 28 days. Particle-induced genotoxicity was assessed in terms of DNA strand break levels by the comet assay. In lung tissue, there were unaltered levels of DNA strand breaks after intratracheal instillation of ZnO, CuO, SnO_2, Al_2O_3, or TiO_2 at either day 1 or 28 post-exposure (Figure 2). In the liver, levels of DNA strand breaks were decreased in mice exposed to the low dose of Al_2O_3 at day 1 (18 μg/mouse, $p < .05$: −1.5% Tail DNA, 95% CI: −2.9, −0.2), whereas they were increased at day 28 in mice exposed to the highest dose of CuO (12 μg/mouse, $p < .05$: 1.5% Tail DNA, 95% CI: 0.03, 3.0). In general, these effects were small and the fact that the effects were observed in opposite directions suggests they may be chance findings. The negative and positive assay controls have levels of DNA strand breaks as follows: 1.4 ± 0.4 for unexposed A549 cells and 23.1 ± 1.2 for H_2O_2-exposed A549 cells (%TDNA, mean ± SD).

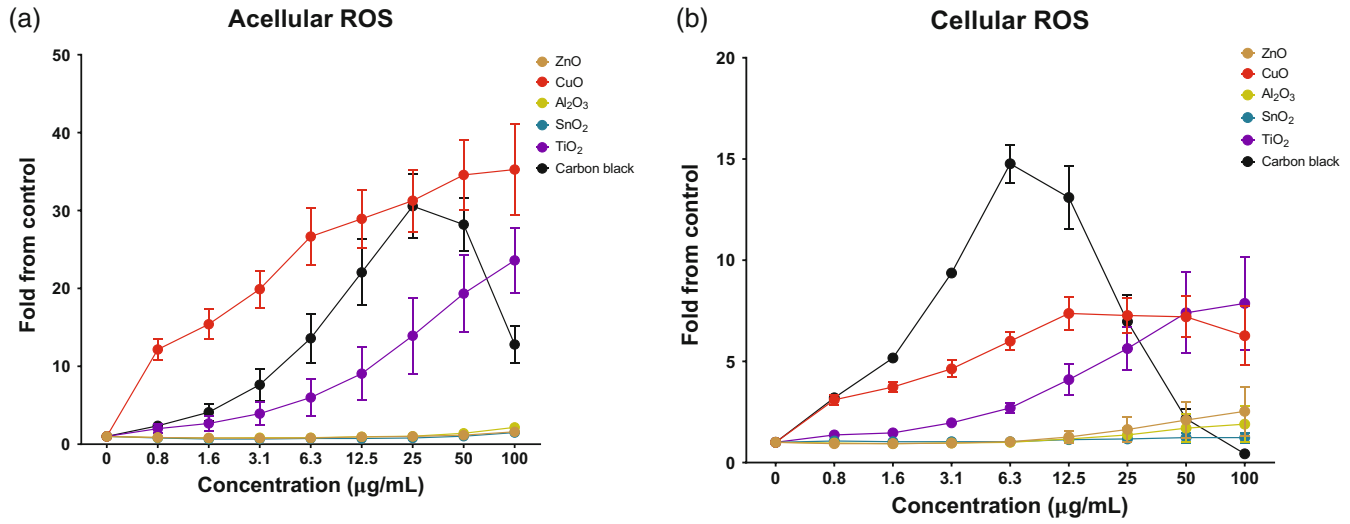

FIGURE 1 Acellular and cellular ROS production after 3 h of exposure to the ZnO, CuO, Al_2O_3, SnO_2, TiO_2, and carbon black nanomaterials. The data are shown as mean ± standard deviation ($N = 3$).

TABLE 2 The slope of acellular and intracellular ROS production by particles.

Sample	Acellular	Cellular
ZnO	−0.02 (−0.05, −0.01)*	0.10 (−0.09, 0.30)
CuO	3.52 (2.47, 4.57)***	0.69 (0.50, 0.88)***
Al_2O_3	−0.02 (−0.04, 0.01)	0.02 (−0.04, 0.01)
SnO_2	−0.03 (−0.61, 0.01)	<0.01 (−0.18, 0.02)
TiO_2	0.77 (0.47, 1.08)***	0.26 (0.22, 0.31)***
Carbon black	2.03 (1.64, 2.42)***	2.18 (2.00, 2.38)***

Note: Initial slope of fold-increase in ROS production (concentration interval from 0 to 6.3 µg/mL). Slopes are based on linear regression (95% confidence intervals are provided in brackets).
*$p < .05$; ***$p < .001$.

4 | DISCUSSION

In the present study, we detected no increases in DNA strand break levels in lung and liver tissue after exposure to metal oxide nanomaterials of CuO, SnO_2, Al_2O_3, ZnO, and TiO_2. Positive and negative assay controls were included in each experiment as quality control of the comet assay. We did not include a positive control for genotoxicity in the animal study because there are no positive control for nanomaterial-induced DNA strand breaks, measured by the comet assay. The OECD test guideline 489 for the in vivo mammalian alkaline comet assay suggests a number of positive controls, such as intraperitoneal administration of direct-acting alkylating (OECD, 2016). However, positive controls are not applicable to certain experimental conditions such as biomonitoring studies, specific routes and modified comet assays for measurement of oxidatively damaged DNA. Thus, recently there has been an incentive to validate assay controls as alternatives to positive controls in situations where the latter is somewhat out of alignment with the experiments (e.g., intraperitoneal injection of a direct-acting alkylating agent in a study protocol on intratracheal administration of nanoparticles; Møller et al., 2018). A relatively large group of researchers who regularly published comet assay results have published recommendations to design and report comet assay results with use of assay controls in situations where true control groups are not applicable (Collins et al., 2023; Møller et al., 2020).

We previously assessed pulmonary inflammation, acute phase response, and protein content and lactate dehydrogenase activity in bronchoalveolar (BAL) fluid as well as histopathological changes in lung tissue in the same study (Gutierrez et al., 2023). We reported that the low solubility particle Al_2O_3 and the insoluble nanomaterials (SnO_2, TiO_2 and carbon black) induced inflammation and acute phase response which was predicted by the deposited surface area. The highly soluble ZnO and CuO induced a stronger inflammatory response per surface area than the insoluble particles. Protein content in BAL fluid correlated with inflammation in terms of neutrophil influx and was significantly increased for SnO_2, TiO_2 and carbon black, all at 162 µg/mouse. Increased lactate dehydrogenase activity in BAL fluid was observed for Al_2O_3 and SnO_2.

Pulmonary exposure to metal oxides induces metal fume fever in a dose-dependent manner (Gordon & Fine, 1993; Hadrup et al., 2020; Schraufnagel, 2020), which entails inflammatory and acute phase responses (Gabay & Kushner, 1999). Metal fume fever flu-like symptoms and weight loss in the mice and even death have been reported at high dose levels of the highly soluble ZnO nanoparticles in mice (Hadrup et al., 2019; Jacobsen et al., 2015). Therefore, dose levels of the metal oxide nanoparticles in the present study were based on in-house pilot studies. The dose levels used in the current study were of occupational relevance. For the highly soluble ZnO, Monsé et al. estimated the pulmonary deposited dose following 2 h exposure at 2 mg/m^3 ZnO nanoparticles to be 0.97 mg per person in a controlled human exposure study (Monsé et al., 2021). This corresponds to

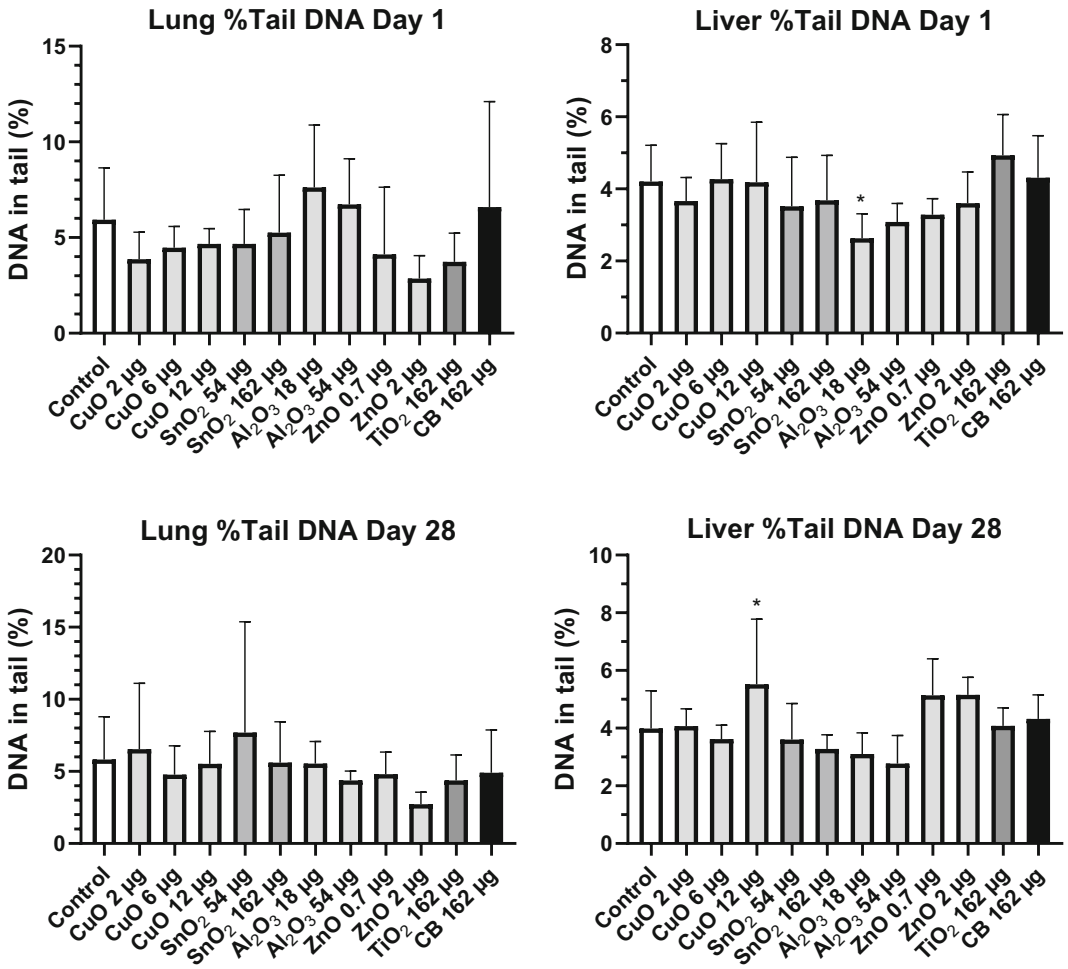

FIGURE 2 Levels of DNA strand breaks in lung and liver tissue at 1 and 28 days post-exposure. Data are mean and bars represent SD. *$p < .05$ relative to the vehicle control (ANOVA). *N* is 6 for the particle groups and *N* is 26 for the control group. CB is an abbreviation of carbon black.

0.97 mg/73 kg = 0.013 mg/kg bw (the average weight of the volunteers was 73 kg). Normalized to an 8 h working day at the occupational exposure limit, this corresponds to 0.013 mg/kg × 8 h/2 h × (5 mg/m^3/2 mg/m^3) = 0.133 mg/kg bw when normalizing to 5 mg/m^3 (the Danish occupational exposure limit) and an 8 h work day. In comparison, mice in the current study had an average weight at exposure of 18.80 ± 0.92 g were exposed to 2 µg ZnO corresponding to 0.106 mg/kg bw. For the insoluble nanoparticles, the dose levels were much higher, and thus, the doses correspond to longer occupational exposures for humans. However, this fits well with the notion that inhaled nanoparticles accumulate in the alveolar region of the lung because the slow clearance from the alveolar region (Elder et al., 2005; Heinrich et al., 1995; Oberdorster et al., 2005). Thus, we have previously estimated that the dose level of 162 µg for carbon black corresponds to a pulmonary deposition after 9 working days for a mouse at the occupational exposure limit of 3.5 mg/m^3 carbon black per 8 h work shift assuming that 33.8% of the inhaled mass ends up in the pulmonary region with a volume of inhaled air per hour of 1.8 L/h (Bourdon et al., 2012). The Danish occupational exposure limits for Al_2O_3 (19 mg/m^3), TiO_2 (10 mg/m^3), and SnO_2 (2.5 mg/m^3) are of similar magnitude as the occupational exposure limit for carbon black as were the dose levels used in the present study. Thus, the dose levels used in the present study were of occupational relevance.

4.1 | ROS production

We assessed acellular and intracellular particle-mediated ROS generation as an indicator of particle reactivity (Boyles et al., 2022), which may contribute to particle-induced genotoxicity (Nymark et al., 2021). The acellular and intracellular ROS measurements were fairly consistent. CuO and the reference particle carbon black were potent ROS generators in both assays, followed by TiO_2. Al_2O_3, ZnO, and SnO_2 generated low levels of ROS. ROS generation has been hypothesized to be an important mechanism of action for carbon black-mediated genotoxicity and mutagenicity (Jacobsen et al., 2011; Modrzynska et al., 2018; Nymark et al., 2021). CuO was also a potent ROS generator in the present study. However, CuO is, similarly to ZnO, highly

soluble in phagolysosomal fluid (Semisch et al., 2014). Thus, CuO undergoes rapid dissolution, releasing Cu+ ions. Thus, CuO is expected to induce short-term effects only. Carbon black (Printex 90) was included as a benchmark nanomaterial, and is known to generate high levels of ROS in both cellular and acellular assays (Jacobsen et al., 2008). Particle-induced ROS has been proposed as a mechanism of action of carbon black-induced genotoxicity (Jacobsen et al., 2011; Modrzynska et al., 2018). However, carbon black nanoparticles are a weak mutagen (Jacobsen et al., 2007) and results in limited genotoxicity in the comet assay (Kyjovska et al., 2015). This material has recently been evaluated in a systematic review (Di Ianni et al., 2022) and although carbon black increased genotoxicity in BAL cells and lung tissue, null reports have also been reported (Barfod et al., 2020; Bendtsen et al., 2019; Bendtsen et al., 2020; Bengtson et al., 2017; Bourdon et al., 2012; Di Ianni et al., 2022; Husain et al., 2013; Kyjovska et al., 2015; Poulsen et al., 2016; Saber et al., 2005).

4.2 | Genotoxicity measurements

We observed a slight effect on DNA damage of the CuO nanomaterial in the liver at the highest dose (Figure 2). We previously assessed the genotoxic potential of CuO particles alone and doped onto silica particles. Genotoxicity was assessed using the comet assay, micronucleus test, and γ-H2AX assay. We observed weak genotoxic effects only in the comet assay. This included effects in lung tissue at the two highest dose levels (4.7 and 14 μg/mouse) of solid 300-nm silica particles with CuO doped onto it 1-day post-exposure, but also with pristine 9.8-nm CuO in the lungs at 0.5 μg/mouse (but not at 1.6 or 4.7 μg/mouse) at the same time point (Hadrup et al., 2021). The in vitro ROS production does not corroborate well with a potential genotoxic effect of CuO nanoparticles in lung tissue of mice, perhaps reflecting the low dose levels in the present study due to pulmonary toxicity. It should be noted that we recently showed that CuO nanoparticles generated DNA strand breaks in THP-1 cells at a rather high concentration (160 μg/mL) as well as genotoxicity in co-cultures of THP-1 and A549 cells (Di Ianni et al., 2024).

We found no genotoxicity in the present study of any of the other metal oxide nanomaterials, TiO_2, Al_2O_3, ZnO, and SnO_2 (Figure 2). We were unable to identify any relevant studies in our literature search regarding the genotoxicity of SnO_2 or Al_2O_3. One study exposing mice by inhalation of 58 or 53 mg/m^3 of ZnO nanoparticles (13 and 36 nm) for 1 h did not show increased genotoxicity by the comet assay (Larsen et al., 2016). We previously investigated the genotoxicity of ZnO nanomaterials by intratracheal instillation. Uncoated (NM-110) and triethoxycaprylylsilane-coated (NM-111) ZnO nanoparticles showed only subtle increases in DNA strand breaks in BAL fluid cells and lung tissue in single-dose groups with no dose–response relationship (Hadrup et al., 2019). Another study showed an increased level of DNA strand breaks in lung tissue in the comet assay at lowest dose level of ZnO nanoparticles tested by intratracheal instillation at 0.23, 0.67, and 2 μg ZnO/mouse (Saber et al., 2022). Collectively, based on our data and the data in the literature, there is some evidence for a genotoxic potential of ZnO nanoparticles, however, additional studies are needed to draw a firm conclusion.

Concerning TiO_2, after 1 h inhalation of 10 nm TiO_2 at 271 mg/m^3, mice lung tissue showed increased levels of DNA strand breaks (Larsen et al., 2016). Brandao et al. investigated a 21-nm TiO_2 nanoparticle by inhalation in rats. The mass concentrations were 0.5, 2, 10, or 50 mg/m^3, 6 h/day for 6 consecutive days. Genotoxicity was increased at the highest exposure level measured by comet assay (Brandão et al., 2021). By contrast, genotoxicity was not increased in mice that inhaled TiO_2 for 4 h/day for 5 days at 0.8, 7.2, or 28.5 mg/m^3. Epithelial lung cells showed no genotoxicity, nor were micronuclei detected in erythrocytes (Lindberg et al., 2012). We previously investigated the effects of TiO_2 nanoparticles in intratracheal instillation studies. Three different TiO_2 nanoparticle types were administered at 67 μg/mouse. The first type had a negative surface charge (NRCWE-001). The second one was modified to be positively charged (NRCWE-002), while the third one was a non-modified rutile TiO_2 (NRCWE-025). NRCWE-025, but not the other two, was genotoxic (Hadrup et al., 2017). Another study investigated NRCWE-001 and NRCWE-002 at doses of 18, 54, and 162 μg/mouse. At 1 and 28 days post-exposure, the level of DNA strand breaks was increased in lung tissue for both particles. At day three, increased genotoxicity in the lung was observed after NRCWE-02 at 18 and 54 μg/mouse. Increased genotoxicity was seen for both particles in the liver and BAL fluid cells, but with no consistent pattern (Wallin et al., 2017). In another study in mice, intratracheal instillation of a 19 nm TiO_2 nanoparticle (54 μg/mouse) did not cause genotoxicity in BAL cells (comet assay), while two coated particles (288 and 21 nm) both induced DNA strand breaks (Saber, Jensen, et al., 2012). Thus, the previous literature points to a genotoxic potential of TiO_2 although there are also negative data, similar to the results obtained in the present study.

4.3 | Conclusion

Genotoxicity is an important toxicological endpoint due to the severity of carcinogenicity as human health issue. We found that CuO nanomaterials and the reference particle carbon black were potent ROS generators in both assays, followed by TiO_2. Al_2O_3, ZnO, and SnO_2 that generated low levels of ROS. The acellular and intracellular ROS measurements were fairly consistent with each other. We detected no increases in genotoxicity measured by the comet assay in mouse lung and liver after pulmonary exposure to CuO, SnO_2, Al_2O_3, ZnO, and TiO_2 nanomaterials at occupationally relevant dose levels, except for a slight effect of CuO in the liver at highest dose. Our results add to the body of evidence for the risk assessment of these metal oxide nanomaterials.

AUTHOR CONTRIBUTIONS

Drs Claudia Torero Gutierrez, Martin Roursgaard, Anne Thoustrup Saber, Peter Møller, and Ulla Vogel designed the study. Drs Claudia Torero Gutierrez and Niels Hadrup analyzed the data and prepared draft figures and tables. Drs Charis Loizides, Iosif Hafez, and George

Biskos produced and characterized the investigated metal oxides. Drs Niels Hadrup, Claudia Torero Gutierrez, and Ulla Vogel prepared the manuscript draft with important intellectual input from all other authors. All authors approved the final manuscript.

ACKNOWLEDGMENTS

Michael Guldbrandsen, Eva Terrida, Anne Abildtrup, Noor Irmam, and Yasmin Akhtar are thanked for their excellent technical assistance.

FUNDING INFORMATION

This work was supported by the Focused Research Effort on Chemicals in the Working Environment (FFIKA) from the Danish Government.

DATA AVAILABILITY STATEMENT

The data that support the findings of this study are available from the corresponding author upon reasonable request.

ORCID

Claudia Torero Gutierrez https://orcid.org/0000-0003-2234-6136
Niels Hadrup https://orcid.org/0000-0002-1188-445X
Martin Roursgaard https://orcid.org/0000-0002-7206-0032
Anne Thoustrup Saber https://orcid.org/0000-0002-7626-709X
Peter Møller https://orcid.org/0000-0002-2021-1249
Ulla Vogel https://orcid.org/0000-0001-6807-1524

REFERENCES

Barfod, K.K., Bendtsen, K.M., Berthing, T., Koivisto, A.J., Poulsen, S.S., Segal, E. et al. (2020) Increased surface area of halloysite nanotubes due to surface modification predicts lung inflammation and acute phase response after pulmonary exposure in mice. *Environmental Toxicology and Pharmacology*, 73, 103266. Available from: https://doi.org/10.1016/j.etap.2019.103266

Bendtsen, K.M., Brostrøm, A., Koivisto, A.J., Koponen, I., Berthing, T., Bertram, N. et al. (2019) Airport emission particles: exposure characterization and toxicity following intratracheal instillation in mice. *Particle and Fibre Toxicology*, 16, 23. Available from: https://doi.org/10.1186/s12989-019-0305-5

Bendtsen, K.M., Gren, L., Malmborg, V.B., Shukla, P.C., Tunér, M., Essig, Y.J. et al. (2020) Particle characterization and toxicity in C57BL/6 mice following instillation of five different diesel exhaust particles designed to differ in physicochemical properties. *Particle and Fibre Toxicology*, 17, 38. Available from: https://doi.org/10.1186/s12989-020-00369-9

Bengtson, S., Knudsen, K.B., Kyjovska, Z.O., Berthing, T., Skaug, V., Levin, M. et al. (2017) Differences in inflammation and acute phase response but similar genotoxicity in mice following pulmonary exposure to graphene oxide and reduced graphene oxide. *PLoS One*, 12, e0178355. Available from: https://doi.org/10.1371/journal.pone.0178355

Bourdon, J.A., Saber, A.T., Jacobsen, N.R., Jensen, K.A., Madsen, A.M., Lamson, J.S. et al. (2012) Carbon black nanoparticle instillation induces sustained inflammation and genotoxicity in mouse lung and liver. *Particle and Fibre Toxicology*, 9, 5. Available from: https://doi.org/10.1186/1743-8977-9-5

Boyles, M., Murphy, F., Mueller, W., Wohlleben, W., Jacobsen, N.R., Braakhuis, H. et al. (2022) Development of a standard operating procedure for the DCFH2-DA acellular assessment of reactive oxygen species produced by nanomaterials. *Toxicology Mechanisms and Methods*, 32, 439–452. Available from: https://doi.org/10.1080/15376516.2022.2029656

Brandão, F., Costa, C., Bessa, M.J., Dumortier, E., Debacq-Chainiaux, F., Hubaux, R. et al. (2021) Genotoxicity and gene expression in the rat lung tissue following instillation and inhalation of different variants of amorphous silica nanomaterials (aSiO2 NM). *Nanomaterials*, 11, 1502. Available from: https://doi.org/10.3390/nano11061502

Chavali, M.S. & Nikolova, M.P. (2019) Metal oxide nanoparticles and their applications in nanotechnology. *SN Applied Sciences*, 1, 607. Available from: https://doi.org/10.1007/s42452-019-0592-3

Collins, A., Møller, P., Gajski, G., Vodenková, S., Abdulwahed, A., Anderson, D. et al. (2023) Measuring DNA modifications with the comet assay: a compendium of protocols. *Nature Protocols*, 18, 929–989. Available from: https://doi.org/10.1038/s41596-022-00754-y

Danielsen, P.H., Knudsen, K.B., Štrancar, J., Umek, P., Koklič, T., Garvas, M. et al. (2020) Effects of physicochemical properties of TiO_2 nanomaterials for pulmonary inflammation, acute phase response and alveolar proteinosis in intratracheally exposed mice. *Toxicology and Applied Pharmacology*, 386, 114830. Available from: https://doi.org/10.1016/j.taap.2019.114830

Di Ianni, E., Erdem, J.S., Narui, S., Wallin, H., Lynch, I., Vogel, U. et al. (2024) Pro-inflammatory and genotoxic responses by metal oxide nanomaterials in alveolar epithelial cells and macrophages in submerged condition and air–liquid interface: an in vitro–in vivo correlation study. *Toxicology in Vitro*, 100, 105897. Available from: https://doi.org/10.1016/j.tiv.2024.105897

Di Ianni, E., Jacobsen, N.R., Vogel, U.B. & Møller, P. (2022) Systematic review on primary and secondary genotoxicity of carbon black nanoparticles in mammalian cells and animals. *Mutation Research, Reviews in Mutation Research*, 790, 108441. Available from: https://doi.org/10.1016/j.mrrev.2022.108441

Elder, A., Gelein, R., Finkelstein, J.N., Driscoll, K.E., Harkema, J. & Oberdörster, G. (2005) Effects of subchronically inhaled carbon black in three species. I. Retention kinetics, lung inflammation, and histopathology. *Toxicological Sciences*, 88, 614–629. Available from: https://doi.org/10.1093/toxsci/kfi327

Feng, J., Biskos, G. & Schmidt-Ott, A. (2015) Toward industrial scale synthesis of ultrapure singlet nanoparticles with controllable sizes in a continuous gas-phase process. *Scientific Reports*, 5, 15788. Available from: https://doi.org/10.1038/srep15788

Gabay, C. & Kushner, I. (1999) Acute-phase proteins and other systemic responses to inflammation. *The New England Journal of Medicine*, 340, 448–454. Available from: https://doi.org/10.1056/NEJM199902113400607

Gordon, T. & Fine, J.M. (1993) Metal fume fever. *Occupational Medicine*, 8, 504–517.

Gutierrez, C.T., Loizides, C., Hafez, I., Brostrøm, A., Wolff, H., Szarek, J. et al. (2023) Acute phase response following pulmonary exposure to soluble and insoluble metal oxide nanomaterials in mice. *Particle and Fibre Toxicology*, 20, 4. Available from: https://doi.org/10.1186/s12989-023-00514-0

Hadrup, N., Aimonen, K., Ilves, M., Lindberg, H., Atluri, R., Sahlgren, N.M. et al. (2021) Pulmonary toxicity of synthetic amorphous silica—effects of porosity and copper oxide doping. *Nanotoxicology*, 15, 96–113. Available from: https://doi.org/10.1080/17435390.2020.1842932

Hadrup, N., Bengtson, S., Jacobsen, N.R., Jackson, P., Nocun, M., Saber, A.T. et al. (2017) Influence of dispersion medium on nanomaterial-induced pulmonary inflammation and DNA strand breaks: investigation of carbon black, carbon nanotubes and three titanium dioxide nanoparticles. *Mutagenesis*, 32, 581–597. Available from: https://doi.org/10.1093/mutage/gex042

Hadrup, N., Rahmani, F., Jacobsen, N.R., Saber, A.T., Jackson, P., Bengtson, S. et al. (2019) Acute phase response and inflammation following pulmonary exposure to low doses of zinc oxide nanoparticles in

mice. *Nanotoxicology*, 13, 1275–1292. Available from: https://doi.org/10.1080/17435390.2019.1654004

Hadrup, N., Sahlgren, N., Jacobsen, N.R., Saber, A.T., Hougaard, K.S., Vogel, U. et al. (2023) Toxicity dose descriptors from animal inhalation studies of 13 nanomaterials and their bulk and ionic counterparts and variation with primary particle characteristics. *Nanotoxicology*, 17, 338–371. Available from: https://doi.org/10.1080/17435390.2023.2221728

Hadrup, N., Zhernovkov, V., Jacobsen, N.R., Voss, C., Strunz, M., Ansari, M. et al. (2020) Acute phase response as a biological mechanism-of-action of (nano)particle-induced cardiovascular disease. *Small*, 16, e1907476. Available from: https://doi.org/10.1002/smll.201907476

Han, B., Pei, Z., Shi, L., Wang, Q., Li, C., Zhang, B. et al. (2020) TiO_2 nanoparticles caused DNA damage in lung and extra-pulmonary organs through ROS-activated FOXO3a signaling pathway after intratracheal administration in rats. *International Journal of Nanomedicine*, 15, 6279–6294. Available from: https://doi.org/10.2147/IJN.S254969

Heinrich, U., Fuhst, R., Rittinghausen, S., Creutzenberg, O., Bellmann, B., Koch, W. et al. (1995) Chronic inhalation exposure of Wistar rats and two different strains of mice to diesel engine exhaust, carbon black, and titanium dioxide. *Inhalation Toxicology*, 7, 533–556.

Husain, M., Saber, A.T., Guo, C., Jacobsen, N.R., Jensen, K.A., Yauk, C.L. et al. (2013) Pulmonary instillation of low doses of titanium dioxide nanoparticles in mice leads to particle retention and gene expression changes in the absence of inflammation. *Toxicology and Applied Pharmacology*, 269, 250–262.

Jackson, P., Lund, S.P., Kristiansen, G., Andersen, O., Vogel, U., Wallin, H. et al. (2011) An experimental protocol for maternal pulmonary exposure in developmental toxicology. *Basic & Clinical Pharmacology & Toxicology*, 108, 202–207. Available from: https://doi.org/10.1111/j.1742-7843.2010.00644.x

Jackson, P., Pedersen, L.M., Kyjovska, Z.O., Jacobsen, N.R., Saber, A.T., Hougaard, K.S. et al. (2013) Validation of freezing tissues and cells for analysis of DNA strand break levels by comet assay. *Mutagenesis*, 28, 699–707. Available from: https://doi.org/10.1093/mutage/get049

Jacobsen, N.R., Pojana, G., White, P., Moller, P., Cohn, C.A., Korsholm, K.S. et al. (2008) Genotoxicity, cytotoxicity, and reactive oxygen species induced by single-walled carbon nanotubes and C(60) fullerenes in the FE1-Mutatrade markMouse lung epithelial cells. *Environmental and Molecular Mutagenesis*, 49, 476–487.

Jacobsen, N.R., Saber, A.T., White, P., Moller, P., Pojana, G., Vogel, U. et al. (2007) Increased mutant frequency by carbon black, but not quartz, in the lacZ and cII transgenes of muta mouse lung epithelial cells. *Environmental and Molecular Mutagenesis*, 48, 451–461.

Jacobsen, N.R., Stoeger, T., van den, B.S., Saber, A.T., Beyerle, A., Vietti, G. et al. (2015) Acute and subacute pulmonary toxicity and mortality in mice after intratracheal instillation of ZnO nanoparticles in three laboratories. *Food and Chemical Toxicology*, 85, 84–95. Available from: https://doi.org/10.1016/j.fct.2015.08.008

Jacobsen, N.R., White, P.A., Gingerich, J., Moller, P., Saber, A.T., Douglas, G.R. et al. (2011) Mutation spectrum in FE1-MUTA (TM) mouse lung epithelial cells exposed to nanoparticulate carbon black. *Environmental and Molecular Mutagenesis*, 52, 331–337.

Kyjovska, Z.O., Jacobsen, N.R., Saber, A.T., Bengtson, S., Jackson, P., Wallin, H. et al. (2015) DNA damage following pulmonary exposure by instillation to low doses of carbon black (Printex 90) nanoparticles in mice. *Environmental and Molecular Mutagenesis*, 56, 41–49.

Larsen, S.T., Jackson, P., Poulsen, S.S., Levin, M., Jensen, K.A., Wallin, H. et al. (2016) Airway irritation, inflammation, and toxicity in mice following inhalation of metal oxide nanoparticles. *Nanotoxicology*, 10, 1254–1262.

Li, Y.-S., Ootsuyama, Y., Kawasaki, Y., Morimoto, Y., Higashi, T. & Kawai, K. (2018) Oxidative DNA damage in the rat lung induced by intratracheal instillation and inhalation of nanoparticles. *Journal of Clinical Biochemistry and Nutrition*, 62, 238–241. Available from: https://doi.org/10.3164/jcbn.17-70

Lindberg, H.K., Falck, G.C., Catalan, J., Koivisto, A.J., Suhonen, S., Jarventaus, H. et al. (2012) Genotoxicity of inhaled nanosized TiO(2) in mice. *Mutation Research*, 745, 58–64.

Modrzynska, J., Berthing, T., Ravn-Haren, G., Jacobsen, N.R., Weydahl, I.K., Loeschner, K. et al. (2018) Primary genotoxicity in the liver following pulmonary exposure to carbon black nanoparticles in mice. *Particle and Fibre Toxicology*, 15, 2. Available from: https://doi.org/10.1186/s12989-017-0238-9

Møller, P., Azqueta, A., Boutet-Robinet, E., Koppen, G., Bonassi, S., Milić, M. et al. (2020) Minimum information for reporting on the comet assay (MIRCA): recommendations for describing comet assay procedures and results. *Nature Protocols*, 15, 3817–3826. Available from: https://doi.org/10.1038/s41596-020-0398-1

Møller, P., Jantzen, K., Løhr, M., Andersen, M.H., Jensen, D.M., Roursgaard, M. et al. (2018) Searching for assay controls for the Fpg- and hOGG1-modified comet assay. *Mutagenesis*, 33, 9–19. Available from: https://doi.org/10.1093/mutage/gex015

Monsé, C., Raulf, M., Jettkant, B., van Kampen, V., Kendzia, B., Schürmeyer, L. et al. (2021) Health effects after inhalation of micro- and nano-sized zinc oxide particles in human volunteers. *Archives of Toxicology*, 95, 53–65. Available from: https://doi.org/10.1007/s00204-020-02923-y

Nymark, P., Karlsson, H.L., Halappanavar, S. & Vogel, U. (2021) Adverse outcome pathway development for assessment of lung carcinogenicity by nanoparticles. *Frontiers in Toxicology*, 3, 653386. Available from: https://doi.org/10.3389/ftox.2021.653386

Oberdorster, G., Oberdorster, E. & Oberdorster, J. (2005) Nanotoxicology: an emerging discipline evolving from studies of ultrafine particles. *Environmental Health Perspectives*, 113, 823–839.

OECD. (2016) OECD guideline for the testing of chemicals. In: *In vivo mammalian alkaline comet assay*. Paris: OCED Publishing. Available from: https://doi.org/10.1787/9789264264885-en

Pfeiffer, T.V., Kedia, P., Messing, M.E., Valvo, M. & Schmidt-Ott, A. (2015) Precursor-less coating of nanoparticles in the gas phase. *Materials*, 8, 1027–1042. Available from: https://doi.org/10.3390/ma8031027

Poulsen, S.S., Jackson, P., Kling, K., Knudsen, K.B., Skaug, V., Kyjovska, Z.O. et al. (2016) Multi-walled carbon nanotube physicochemical properties predict pulmonary inflammation and genotoxicity. *Nanotoxicology*, 10, 1263–1275.

Saber, A.T., Bornholdt, J., Dybdahl, M., Sharma, A.K., Loft, S., Vogel, U. et al. (2005) Tumor necrosis factor is not required for particle-induced genotoxicity and pulmonary inflammation. *Archives of Toxicology*, 79, 177–182.

Saber, A.T., Hadrup, N., Williams, A., Mortensen, A., Szarek, J., Kyjovska, Z. et al. (2022) Unchanged pulmonary toxicity of ZnO nanoparticles formulated in a liquid matrix for glass coating. *Nanotoxicology*, 16, 812–827. Available from: https://doi.org/10.1080/17435390.2022.2152751

Saber, A.T., Jacobsen, N.R., Mortensen, A., Szarek, J., Jackson, P., Madsen, A.M. et al. (2012) Nanotitanium dioxide toxicity in mouse lung is reduced in sanding dust from paint. *Particle and Fibre Toxicology*, 9, 4.

Saber, A.T., Jensen, K.A., Jacobsen, N.R., Birkedal, R., Mikkelsen, L., Moller, P. et al. (2012) Inflammatory and genotoxic effects of nanoparticles designed for inclusion in paints and lacquers. *Nanotoxicology*, 6, 453–471.

Schraufnagel, D.E. (2020) The health effects of ultrafine particles. *Experimental & Molecular Medicine*, 52, 311–317. Available from: https://doi.org/10.1038/s12276-020-0403-3

Schwyn, S., Garwin, E. & Schmidt-Ott, A. (1988) Aerosol generation by spark discharge. *Journal of Aerosol Science*, 19, 639–642. Available from: https://doi.org/10.1016/0021-8502(88)90215-7

Semisch, A., Ohle, J., Witt, B. & Hartwig, A. (2014) Cytotoxicity and genotoxicity of nano- and microparticulate copper oxide: role of solubility and intracellular bioavailability. *Particle and Fibre Toxicology*, 11, 10. Available from: https://doi.org/10.1186/1743-8977-11-10

Wallin, H., Kyjovska, Z.O., Poulsen, S.S., Jacobsen, N.R., Saber, A.T., Bengtson, S. et al. (2017) Surface modification does not influence the genotoxic and inflammatory effects of TiO_2 nanoparticles after pulmonary exposure by instillation in mice. *Mutagenesis*, 32, 47–57.

SUPPORTING INFORMATION

Additional supporting information can be found online in the Supporting Information section at the end of this article.

How to cite this article: Gutierrez, C.T., Hadrup, N., Loizides, C., Hafez, I., Biskos, G., Roursgaard, M. et al. (2024) Absence of genotoxicity following pulmonary exposure to metal oxides of copper, tin, aluminum, zinc, and titanium in mice. *Environmental and Molecular Mutagenesis*, 65(8), 251–260. Available from: https://doi.org/10.1002/em.22634